

Supporting information for

A *trans*-bidentate *bis*-pyridinyl ligand with a transition metal hinge

Noah C. Vieira,^a Jared A. Pienkos,^{*a} Colin D. McMillen,^b Alexis R. Myers,^a Alyssa P. Clay,^a
Paul S. Wagenknecht.^{*a}

^a*Department of Chemistry, Furman University, Greenville, SC, 29613, USA.* ^b*Department of Chemistry, Clemson University, Clemson, SC, 29534, USA.*

	Page
General Methods	S2
Experimental Procedures	S2-S4
Table S1: Crystallographic data for complexes 1-3 .	S5
Figure S1: Comparison of three different orientations for complexes 1-3 .	S6
Figure S2: Packing arrangement in 1 .	S7
Figure S3: Packing arrangement in 2 .	S7
Figure S4: Packing arrangement in 3 .	S8
Figure S5: UV-Visible Spectra in CH ₂ Cl ₂ .	S8
Figure S6: Cyclic Voltammograms in CH ₂ Cl ₂ .	S9
Figure S7: ¹ H- and ¹³ C-NMR spectra of Cp* ₂ Ti(C ₂ 2-py) ₂ (1).	S10
Figure S8: ¹ H- and ¹³ C-NMR spectra of Cp* ₂ Ti(C ₂ 2-py) ₂ Cu(OH ₂)PF ₆ (2).	S11
Figure S9: ¹ H- and ¹³ C-NMR spectra of Cp* ₂ Ti(C ₂ 2-py) ₂ PdCl ₂ (3).	S12
References	S13

General Methods

THF, Et₂O, and CH₂Cl₂ were dried and degassed using an Innovative Technology Inc. solvent purification system before use. All other materials were reagent grade and used as received. Reactions were performed under a dry Ar atmosphere implementing standard Schlenk procedures unless otherwise noted. UV-Visible absorption spectra were recorded using a Cary-50 spectrophotometer. NMR spectra were obtained using a Varian 400-MR or an INOVA 500 spectrometer. Infrared spectra were measured on solid samples using a Perkin-Elmer Spectrum 100 series FT-IR spectrometer equipped with an ATR accessory. Cyclic voltammograms were recorded using a BASi Epsilon electrochemical workstation and a BASi cell stand. Elemental analyses were performed by Midwest Microlabs in Indianapolis, IN.

Experimental Procedures

*Cp*₂Ti(C₂2-py)₂*. (1) To an oven-dried 100 mL two-neck round-bottom flask under a positive pressure of argon was added Et₂O (40 mL) and 2-ethynylpyridine (0.49 mL, 4.85 mmol). After the pale-yellow solution was cooled in a dry ice/acetone bath for 10 min, n-butyllithium (2.5 M, 1.94 mL, 4.85 mmol) was added. The solution was stirred in the bath for 10 min and then was removed for 10 min. Cp*₂TiCl₂ (924 mg, 2.37 mmol) was added and the mixture was allowed to stir at room temperature in the absence of light for 4 h. The following workup was performed without the need of an inert atmosphere and with minimal light exposure to avoid degradation of **1**. The reaction mixture was concentrated and loaded onto a triethylamine treated silica gel column (2.5 x 12 cm) and eluted using a 5% solution of triethylamine in CH₂Cl₂. A dark-red band was collected and the solvent was then removed using rotary evaporation. The resulting solid was dissolved in minimal THF (approximately 5 mL), precipitated with hexanes (approximately 50 mL), collected using vacuum filtration, and dried under vacuum, yielding 812 mg (65.5%) of a purple powder. UV/Vis (THF), λ/nm (ε/dm³ mol⁻¹ cm⁻¹): 475 (2505), 363 (sh, 13,238). ¹H NMR (500 MHz, CDCl₃) δ 8.52 (ddd, *J* = 4.9, 1.8, 0.9, 2H), 7.51 (td, *J* = 7.7, 1.9 Hz, 2H), 7.25 (dt, *J* = 7.9, 1.1, 2H), 7.01 (ddd, *J* = 7.5, 4.9, 1.2, 2H), 2.09 (s, 30H); ¹³C {¹H} NMR (400 MHz, CDCl₃) δ 161.4, 149.8, 146.2, 135.6, 126.1, 124.2, 122.3, 120.4, 13.3. Anal. Calcd (found) for C₃₄H₃₈N₂Ti: C, 77.89 (78.15); H, 7.15 (7.33); N, 5.27 (5.36). IR (neat) ν_{C≡C} = 2077 cm⁻¹.

*Cp*₂Ti(C₂2-py)₂CuOH₂PF₆*. (2) To an oven-dried two-neck round-bottom flask under a positive pressure of argon was added CH₂Cl₂ (60 mL) and Cp*₂Ti(C₂2-py)₂ (150 mg, 0.29 mmol). After the dark-red solution was stirred at room temperature for 5 min, Cu(CH₃CN)₄PF₆ (107 mg, 0.29 mmol) was added and the mixture was allowed to stir at room temperature in the absence of light for 1 h. After Cu(I) insertion, the following workup was performed under ambient lighting without the need of an inert atmosphere. The solvent was removed and the resulting solid was dried under vacuum

for 1 h. The product was dissolved in minimal CH₂Cl₂ (approximately 15 mL), precipitated with hexanes (approximately 70 mL), collected using vacuum filtration, and dried under vacuum, yielding 120 mg (57.8%) of an orange powder. UV/Vis (THF), λ/nm (ε/dm³ mol⁻¹ cm⁻¹): 465 (sh, 755), 335 (sh, 14,494). ¹H NMR (500 MHz, CDCl₃) δ 8.60 (d, *J* = 4.0 Hz, 2H), 7.85 (t, *J* = 7.6 Hz, 2H), 7.61 (d, *J* = 7.9 Hz, 2H), 7.35 (t, *J* = 6.1, 2H), 6.48 (bs, 2H), 1.97 (s, 30H); ¹³C {¹H} NMR (400 MHz, CDCl₃) δ 151.7, 148.9, 143.8, 138.4, 128.1, 126.0, 123.7, 123.5, 13.0. Anal. Calcd (found) for C₃₄H₄₀N₂OCuTiPF₆ • H₂O: C, 53.24 (53.40); H, 5.52 (5.30); N, 3.65 (3.64). IR (neat) ν_{C=C} = 1958 cm⁻¹.

*Cp**₂Ti(C₂-py)₂PdCl₂. (**3**) To an oven-dried two-neck round-bottom flask under a positive pressure of argon was added CH₂Cl₂ (3 mL) and *Cp**₂Ti(C₂-py)₂ (143 mg, 0.27 mmol). After the dark-red solution was stirred at room temperature for 5 min, Pd(CH₃CN)₂Cl₂ (88 mg, 0.34 mmol) in CH₃CN (12 mL) was transferred by cannula and the mixture was allowed to stir at room temperature in the absence of light for 18 h. After Pd(II) insertion, the following workup was performed under ambient lighting without the need of an inert atmosphere. The solvent was removed by rotary evaporation. The resulting solid was sonicated in CH₃CN (5mL) and filtered using vacuum filtration. The solid was collected and loaded onto a triethylamine treated silica gel column (1 x 20 cm) and eluted using a 5% solution of triethylamine in CH₂Cl₂. The solvent was then removed using rotary evaporation. A light red band was collected and the solvent was removed using rotary evaporation. The resulting solid was dissolved in minimal THF (approximately 2 mL), precipitated with hexanes (approximately 50 mL), collected using vacuum filtration, and dried under vacuum, yielding 55.1 mg (28.8%) of a pink powder. UV/Vis (THF), λ/nm (ε/dm³ mol⁻¹ cm⁻¹): 475 (sh, 1948), 350 (sh, 16,765). ¹H NMR (500 MHz, CDCl₃) δ 8.64 (ddd, *J* = 5.8, 1.6, 0.7, 2H), 7.48 (td, *J* = 7.7, 1.6 Hz, 2H), 7.11 (ddd, *J* = 8.0, 1.5, 0.7, 2H), 7.00 (ddd, *J* = 7.4, 5.8, 1.5, 2H), 2.12 (s, 30H); ¹³C {¹H} NMR (400 MHz, CDCl₃) δ 173.3, 152.2, 147.1, 137.1, 126.0, 124.9, 121.1, 116.8, 13.2. Anal. Calcd (found) for C₃₄H₃₈N₂TiPdCl₂ • H₂O: C, 57.13 (56.89); H, 5.53 (5.62); N, 3.93 (3.90). IR (neat) ν_{C=C} = 2079 cm⁻¹.

X-ray Crystallography. For **1** and **3**, crystals suitable for diffraction were grown from THF by slow evaporation. Crystals of **2** were grown by layering hexanes onto a solution of **2** in CH₂Cl₂. The crystal structures were determined by single crystal X-ray diffraction measured using a Bruker D8 Venture diffractometer. Crystals were mounted on a low-scatter loop using paratone, and immediately cooled to 100 ± 2 K in a cold nitrogen gas stream. Data were collected by phi and omega scans using Mo Kα (λ = 0.71073 Å) radiation from an Incoatec microfocus source, and a Photon 100 detector. Data were processed and scaled (multi-scan absorption correction) using the SAINT and SADABS routines in the Apex3 software suite.¹ The space groups were determined based on the systematic absences, and the structures were solved by intrinsic phasing (SHELXT) and subsequently refined by Fourier difference techniques using full-matrix-least-squares on *F*² (SHELXL) using the SHELXTL package.² All non-hydrogen atoms were refined anisotropically. Hydrogen atoms attached to carbon atoms were placed in

geometrically idealized positions and refined using appropriate riding models. In the case of the coordinated H₂O molecule in **2**, the hydrogen atoms were identified from the difference electron density map, and their positions freely refined using appropriate distance fixing restraints. Here, the hydrogen atoms of the water molecule and the nitrogen atoms of the pyridinyl groups were oriented in favorable positions for intramolecular hydrogen bonding, with D-H...A distances of 2.689(11)-2.790(2) Å.

Several instances of disorder were included in the models of **1-3**. In **1**, one of the Cp* groups attached to the Ti center was found to exhibit a rotational disorder. The two components were distinguished from the difference electron density map and their occupancies freely refined in approximately 62:38 ratio. The majority ratio was selected for the graphical renderings in the manuscript and SI. The fluorine atoms of the [PF₆]⁻ counterion of **2** were also found to be disordered, and their occupancies freely refined. In the case of **3**, a disordered acetonitrile solvent molecule was found to cocrystallize with the target complex, and two partially-occupied arrangements were modeled in disorder about an inversion center. Details of the data collection and refinements are summarized in Table S1. In addition to the thermal ellipsoid plots in the manuscript, a comparison of the molecular geometries, as well as additional packing diagrams are included as Figures S1-S4 here in the Supporting Information.

Table S1: Crystallographic data for complexes **1-3**.

	1 C ₃₄ H ₃₈ N ₂ Ti	2 [C ₃₄ H ₄₀ CuN ₂ OTi][PF ₆]	3 C ₃₄ H ₃₈ Cl ₂ N ₂ PdTi · 0.5(CH ₃ CN)
CCDC reference no.	1571228	1571229	1571227
Formula weight (g/mol)	522.56	749.09	720.39
Temperature (K)	100(2) K	100(2)	100(2)
Wavelength (Å)	0.71073 Å	0.71073	0.71073
Crystal system, space group	Monoclinic, <i>P</i> 2 ₁ / <i>c</i>	Monoclinic, <i>P</i> 2 ₁ / <i>n</i>	Triclinic, <i>P</i> -1
<i>a</i> , Å	10.3807(12)	14.5015(7)	8.8432(3)
<i>b</i> , Å	16.385(2)	15.9769(8)	12.3352(5)
<i>c</i> , Å	16.9043(19)	15.0401(7)	16.4088(7)
α , °	90	90	104.000(2)
β , °	101.544(4)	105.672(2)	93.8680(10)
γ , °	90	90	96.8550(10)
<i>V</i> , Å ³	2817.1(6)	3355.1(3)	1715.69(12)
<i>Z</i> , D _{cal} g/cm ³	4, 1.232	4, 1.483	2, 1.394
μ , mm ⁻¹	0.329	0.983	0.939
<i>F</i> (000)	1112	1544	738
Crystal size, mm	0.191 × 0.204 × 0.208	0.131 × 0.142 × 0.541	0.031 × 0.031 × 0.322
Theta range for data collection	2.36 to 25.25	1.94 to 26.50°	2.33 to 26.07°
Index ranges	-12 ≤ <i>h</i> ≤ 12 -19 ≤ <i>k</i> ≤ 19 -20 ≤ <i>l</i> ≤ 20	-18 ≤ <i>h</i> ≤ 18 -20 ≤ <i>k</i> ≤ 20 -18 ≤ <i>l</i> ≤ 18	-10 ≤ <i>h</i> ≤ 10 -15 ≤ <i>k</i> ≤ 15 -20 ≤ <i>l</i> ≤ 20
Reflections collected	48697	102006	27680
Independent reflections	5104 [R(int) = 0.0750]	6942 [R(int) = 0.0421]	6778 [R(int) = 0.0441]
Max. and min. transmission	1.0000 and 0.9619	1.0000 and 0.8431	1.0000 and 0.9371
Data / restraints / parameters	5104 / 192 / 440	6942 / 95 / 495	6778 / 82 / 427
Goodness-of-fit on <i>F</i> ²	1.060	1.173	1.042
Final <i>R</i> indices [<i>I</i> > 2 σ(<i>I</i>)]	<i>R</i> 1 = 0.0684 <i>wR</i> 2 = 0.1756	<i>R</i> 1 = 0.0289 <i>wR</i> 2 = 0.0802	<i>R</i> 1 = 0.0376 <i>wR</i> 2 = 0.1009
<i>R</i> indices (all data)	<i>R</i> 1 = 0.0893 <i>wR</i> 2 = 0.1922	<i>R</i> 1 = 0.0353 <i>wR</i> 2 = 0.0937	<i>R</i> 1 = 0.0520 <i>wR</i> 2 = 0.1100
Largest diff. peak and hole (e·Å ⁻³)	1.050 and -0.394	0.657 and -0.846	0.993 and -0.881

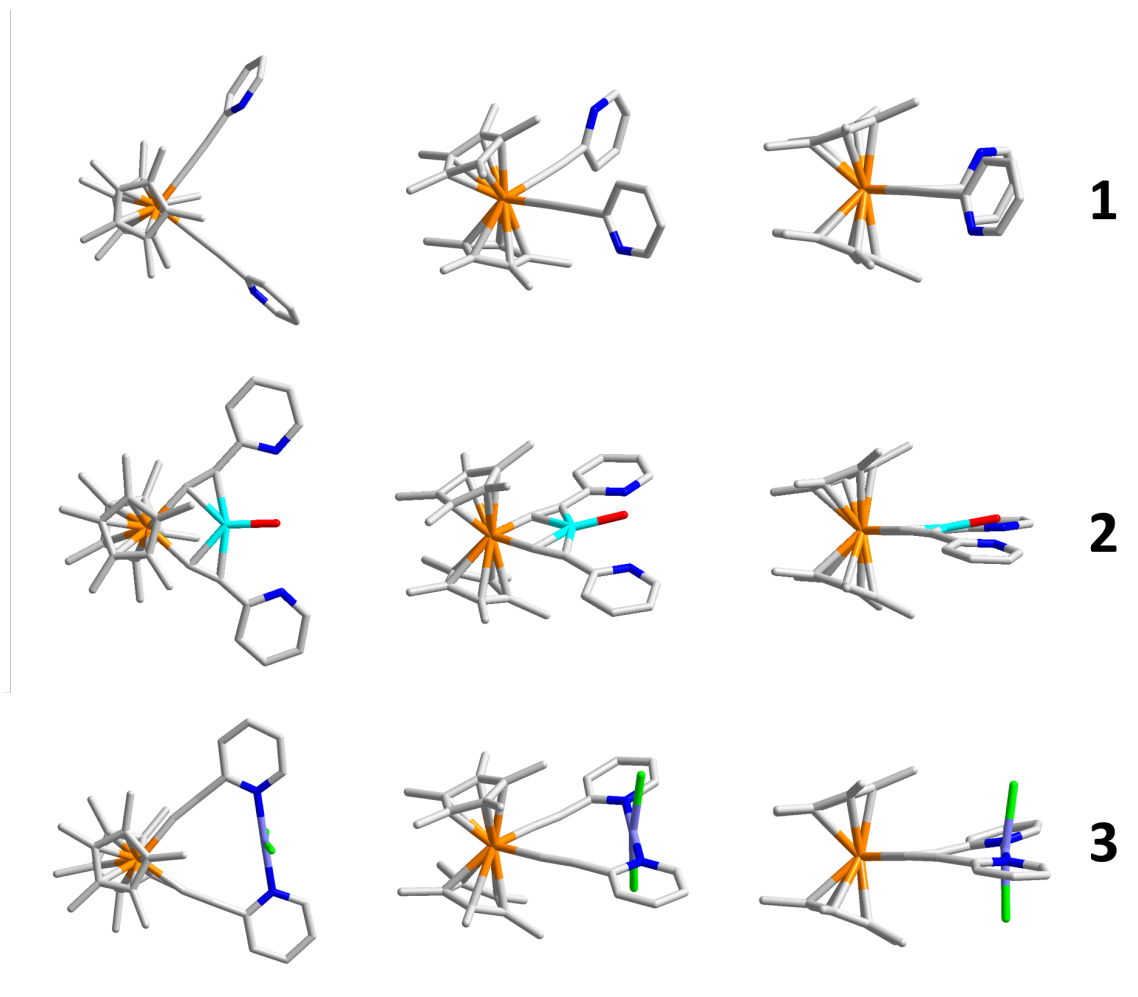


Figure S1: Comparison of three different orientations of the Ti-hinged *trans*-bidentate *bis*-pyridinyl ligand (**1**), the bimetallic Cu(I) complex (**2**), and the bimetallic Pd(II) complex (**3**) of the present study. Wireframe color scheme: Orange = Ti, cyan = Cu, purple = Pd, green = Cl, red = O, blue = N, silver = C; hydrogen atoms omitted for clarity.

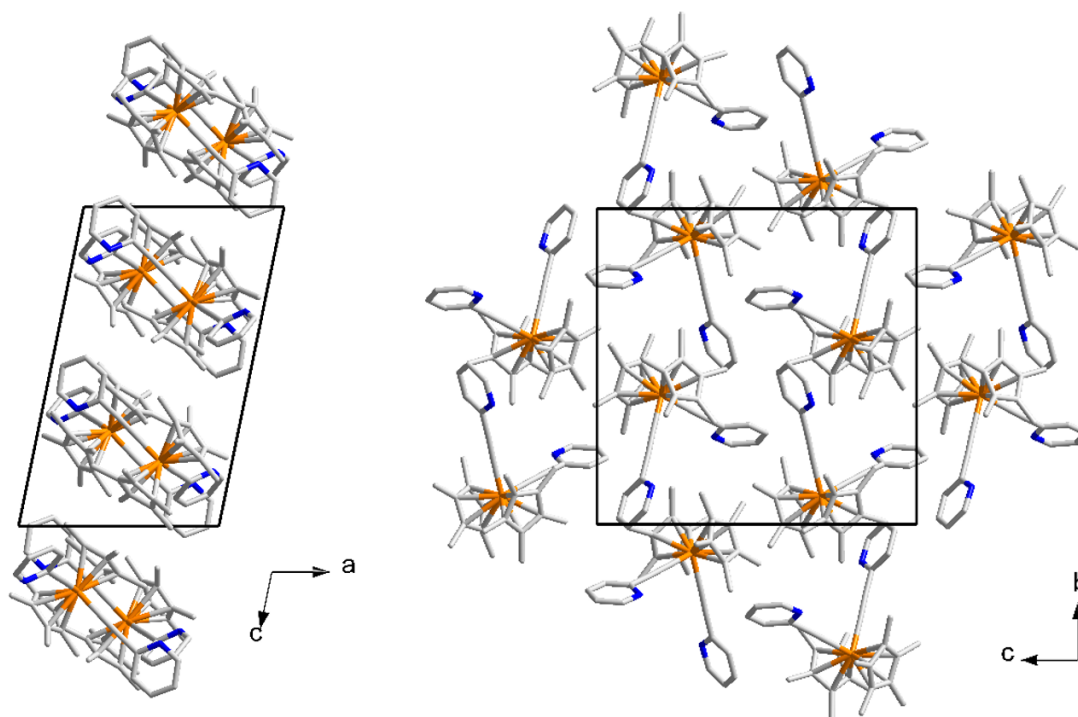


Figure S2: Packing arrangement in **1** along [010] (left) and [100] (right) projections. Wireframe color scheme: Orange = Ti, blue = N, silver = C; hydrogen atoms omitted for clarity.

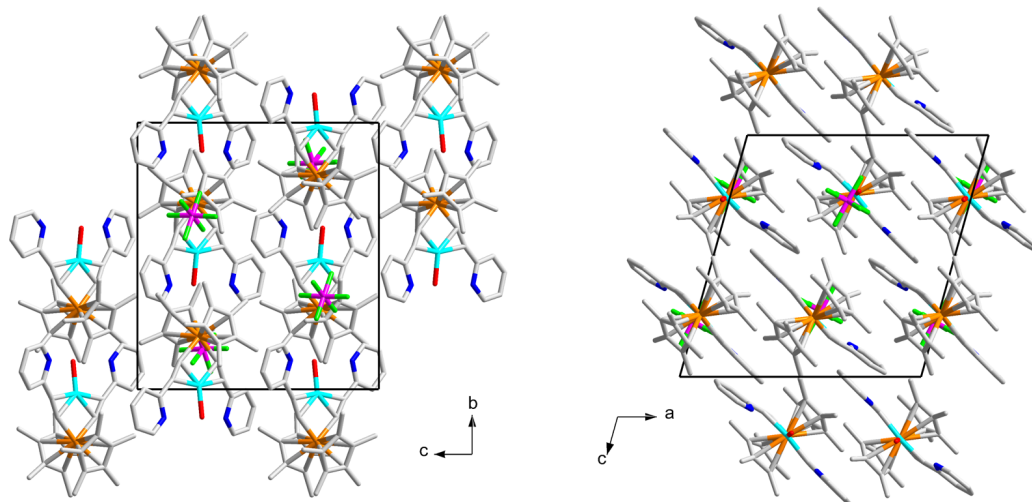


Figure S3: Packing arrangement in **2** along [100] (left) and [010] (right) projections. Wireframe color scheme: Orange = Ti, cyan = Cu, pink = P, green = F, red = O, blue = N, silver = C; hydrogen atoms omitted for clarity.

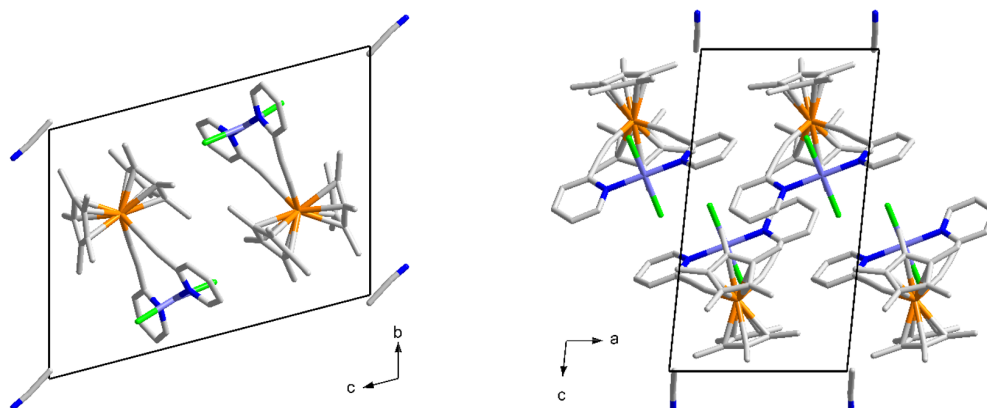


Figure S4: Packing arrangement in **3** along [100] (left) and [010] (right) projections. Wireframe color scheme: Orange = Ti, purple = Pd, green = Cl, blue = N, silver = C; hydrogen atoms omitted for clarity.

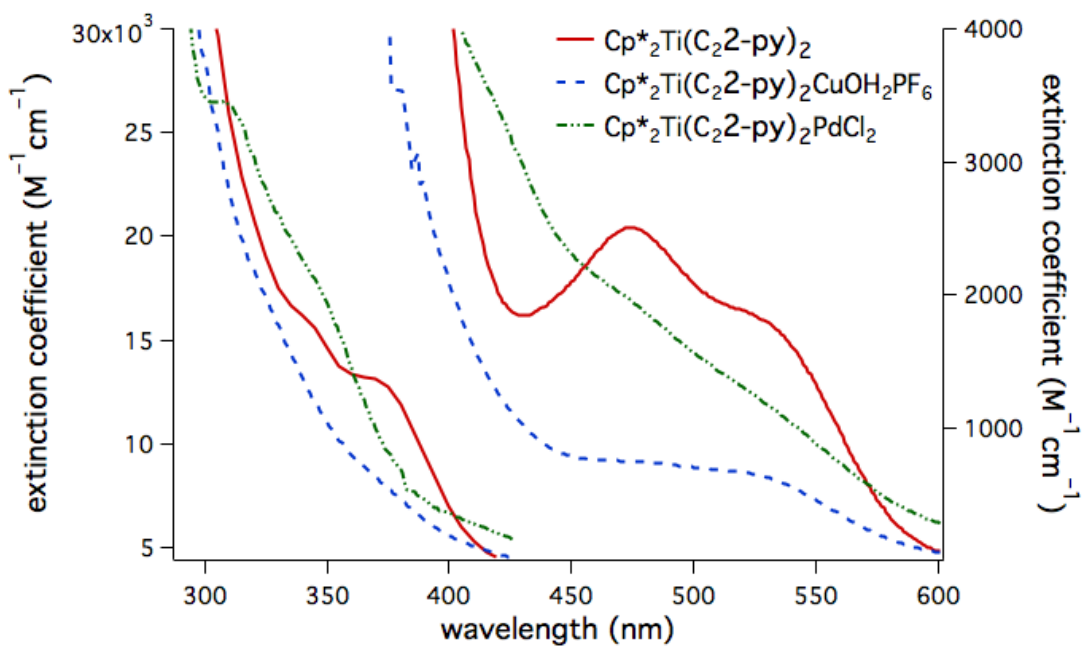


Figure S5: UV-Visible Spectra in CH_2Cl_2 .

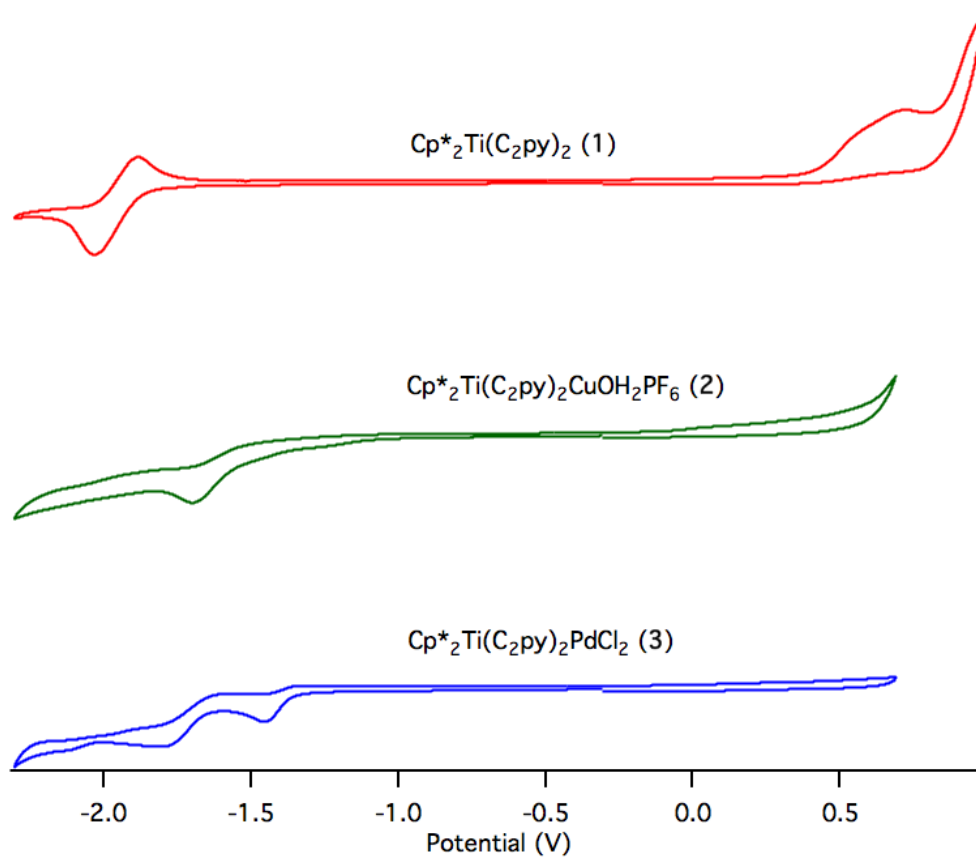


Figure S6: Cyclic voltammogram in CH_2Cl_2 . Conditions: $[\text{Ti}] \sim 1\text{mM}$ in CH_2Cl_2 (0.1 M TBAP), Pt working electrode, Ag/Ag^+ reference electrode. The x-axis reports voltages vs. $\text{FcH}^{+/0}$ as determined by running a voltammogram of $\text{FcH}^{+/0}$ before and after data collection.

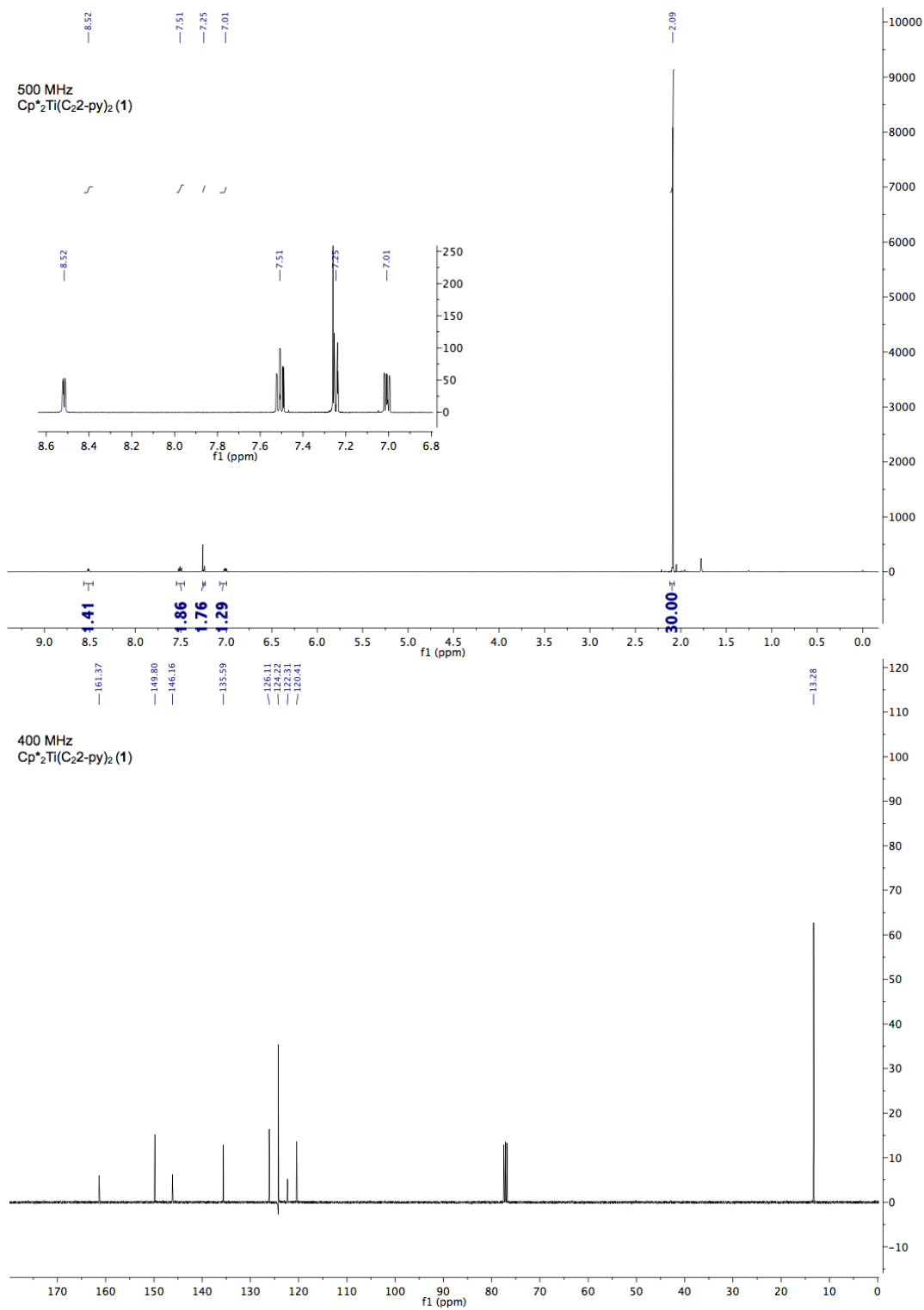


Figure S7: ¹H-NMR (500 MHz, top) and ¹³C-NMR (400 MHz, bottom) of Cp*₂Ti(C₂2-py)₂ (**1**).

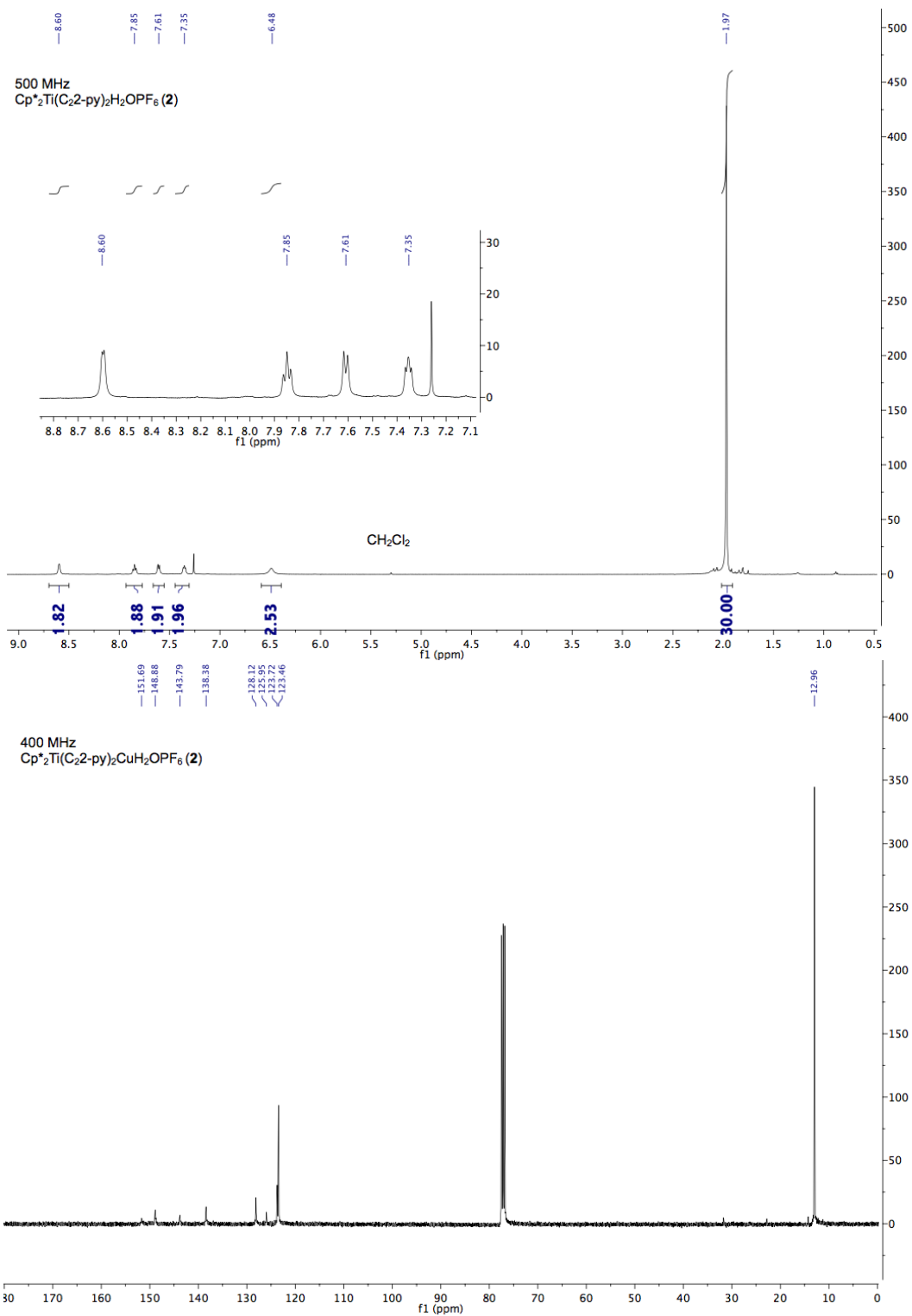


Figure S8: ^1H -NMR (500 MHz, top) and ^{13}C -NMR (400 MHz, bottom) of $\text{Cp}^*_2\text{Ti}(\text{C}_2\text{2-py})_2\text{OH}_2\text{PF}_6$ (**2**).

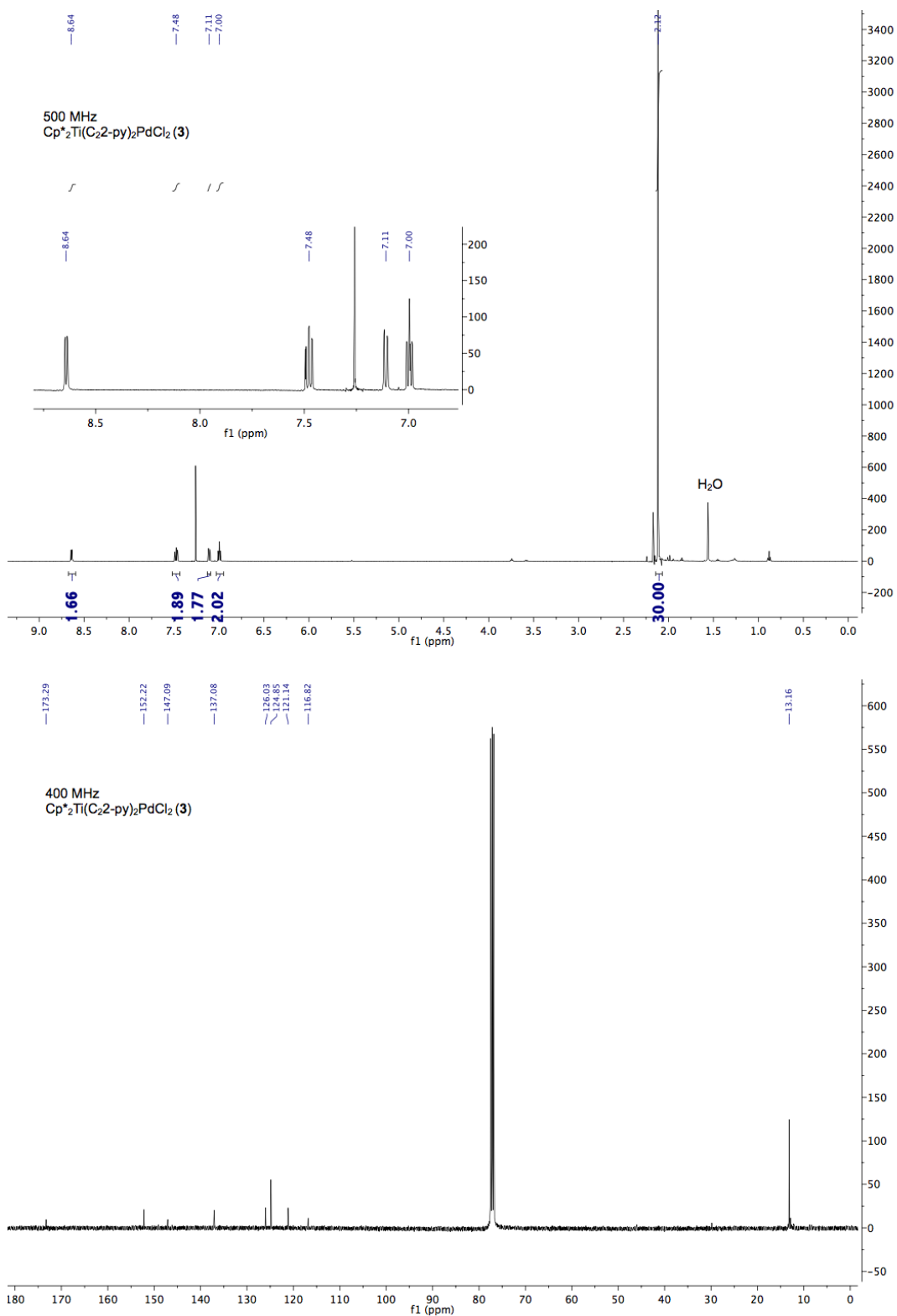


Figure S9: ¹H-NMR (500 MHz, top) and ¹³C-NMR (400 MHz, bottom) of Cp*₂Ti(C₂2-py)₂PdCl₂ (3).

References:

1. Apex 3, **2015**, Bruker AXS, Inc.: Madison, WI.
2. G. Sheldrick, *Acta Crystallogr.*, 2008, **A64**, 112-122.